

AD-A242 831



OFFICE OF NAVAL RESEARCH

GRANT N00014-89-J-1178

R&T Code 413Q001-05

TECHNICAL REPORT NO. #41

A Spectroscopic Immersion Ellipsometry Study Of The
Mechanism Of Si/SiO₂ Interface Annealing

by

V. A. Yakovlev, Q. Liu and E. A. Irene
Department of Chemistry, CB# 3290
University of North Carolina
Chapel Hill, NC 27599-3290

Submitted to the
Journal of Vacuum Science and Technology A

Reproduction in whole or in part is permitted for any purpose of the United States Government.

This document has been approved for public release and sale; its distribution is unlimited.

91-16643



01 11 8 2

REPORT DOCUMENTATION PAGE

1a. REPORT SECURITY CLASSIFICATION unclassified		1b. RESTRICTIVE MARKINGS													
2a. SECURITY CLASSIFICATION AUTHORITY		3. DISTRIBUTION/AVAILABILITY OF REPORT Approved for public release; distribution unlimited.													
2b. DECLASSIFICATION/DOWNGRADING SCHEDULE															
4. PERFORMING ORGANIZATION REPORT NUMBER(S) Technical Report #41		5. MONITORING ORGANIZATION REPORT NUMBER(S)													
6a. NAME OF PERFORMING ORGANIZATION UNC Chemistry Department	6b. OFFICE SYMBOL (If applicable)	7a. NAME OF MONITORING ORGANIZATION Office of Naval Research (Code 413)													
6c. ADDRESS (City, State and ZIP Code) CB# 13290, Venable Hall University of North Carolina Chapel Hill, NC 27599-3290		7b. ADDRESS (City, State and ZIP Code) Chemistry Program 800 N. Quincy Street Arlington, Virginia 22217													
8a. NAME OF FUNDING/SPONSORING ORGANIZATION Office of Naval Research	8b. OFFICE SYMBOL (If applicable)	9. PROCUREMENT INSTRUMENT IDENTIFICATION NUMBER Grant #N00014-89-J-1178													
8c. ADDRESS (City, State and ZIP Code) Chemistry Program 800 N. Quincy Street, Arlington, VA 22217		10. SOURCE OF FUNDING NOS <table border="1"> <thead> <tr> <th>PROGRAM ELEMENT NO</th> <th>PROJECT NO</th> <th>TASK NO</th> <th>WORK UN NO</th> </tr> </thead> <tbody> <tr> <td></td> <td></td> <td></td> <td></td> </tr> </tbody> </table>		PROGRAM ELEMENT NO	PROJECT NO	TASK NO	WORK UN NO								
PROGRAM ELEMENT NO	PROJECT NO	TASK NO	WORK UN NO												
11. TITLE (Include Security Classification) A SPECTROSCOPIC IMMERSSION ELLIPSOMETRY STUDY OF THE MECHANISM OF Si/SiO₂ INTERFACE ANNEALING															
12. PERSONAL AUTHOR(S) V. A. Yakovlev*, Q. Liu and E. A. Irene															
13a. TYPE OF REPORT Interim Technical	13b. TIME COVERED FROM _____ TO _____	14. DATE OF REPORT (Yr, Mo, Day) November 1991	15. PAGE COUNT 32												
16. SUPPLEMENTARY NOTATION Journal of the Vacuum Science Technology A															
17. COSATI CODES <table border="1"> <thead> <tr> <th>FIELD</th> <th>GROUP</th> <th>SUB. GR.</th> </tr> </thead> <tbody> <tr> <td></td> <td></td> <td></td> </tr> <tr> <td></td> <td></td> <td></td> </tr> <tr> <td></td> <td></td> <td></td> </tr> </tbody> </table>		FIELD	GROUP	SUB. GR.										18. SUBJECT TERMS (Continue on reverse if necessary and identify by block number)	
FIELD	GROUP	SUB. GR.													
19. ABSTRACT (Continue on reverse if necessary and identify by block number) <p>In this study we apply an interface sensitive ellipsometry technique to study the evolution of the Si-SiO₂ interface as a function of high temperature annealing (750°-1100°C). Essentially, the ellipsometry technique embodies the use of liquids that refractive index match with the bulk film thereby removing the optical response of the overlayer and greatly enhancing sensitivity to the interface. According to both time and temperature of anneal, distinct modes of behavior are observed for the evolution of the interface. For short anneal times a rapid change in the interface is observed that correlates with the disappearance of protrusions, followed by a slower change that correlates with the disappearance of the suboxide. At high temperatures viscous relaxation dominates while at low temperatures the suboxide reduction is apparent. A model for the interface in terms of chemical and physical interface processes is proposed and model parameters are compared with literature results.</p>															
20. DISTRIBUTION/AVAILABILITY OF ABSTRACT UNCLASSIFIED/UNLIMITED <input checked="" type="checkbox"/> SAME AS RPT <input type="checkbox"/> DTIC USERS <input type="checkbox"/>		21. ABSTRACT SECURITY CLASSIFICATION Unclassified													
22a. NAME OF RESPONSIBLE INDIVIDUAL Dr. Mark Ross		22b. TELEPHONE NUMBER (Include Area Code) (202) 696-4410	22c. OFFICE SYMBOL												

41

A Spectroscopic Immersion Ellipsometry Study of the Mechanism of
Si/SiO₂ Interface Annealing

V.A.Yakovlev*, Q. Liu and E.A.Irene
Department of Chemistry
University of North Carolina at Chapel Hill
Chapel Hill, NC 25799-3290

* Institute of Crystallography, Acad. of Sci. of the USSR,
Leninsky pr., 59 Moscow 117333 USSR

Abstract

In this study we apply an interface sensitive ellipsometry technique to study the evolution of the Si-SiO₂ interface as a function of high temperature annealing (750°-1100°C). Essentially, the ellipsometry technique embodies the use of liquids that refractive index match with the bulk film thereby removing the optical response of the overlayer and greatly enhancing sensitivity to the interface. According to both time and temperature of anneal, distinct modes of behavior are observed for the evolution of the interface. For short anneal times a rapid change in the interface is observed that correlates with the disappearance of protrusions, followed by a slower change that correlates with the disappearance of the suboxide. At high temperatures viscous relaxation dominates while at low temperatures the suboxide reduction is apparent. A model for the interface in terms of chemical and physical interface processes is proposed and model parameters are compared with literature results.

Introduction

The Si/SiO₂ interface continues to be a topic of intensive study. Of particular importance are properties of the interface such as structure, thickness, uniformity and phase composition which have been explored by numerous methods including transmission electron microscopy, TEM (1-2), infrared spectroscopy (3), low-energy electron diffraction (4), scanning tunneling microscopy (5), ellipsometry (6-10), and a variety of surface spectroscopies (11). Presently, ultra-thin SiO₂ films (thickness less than 30 nm) find extensive application in submicron integrated circuit technology where even a small degree of interfacial microroughness or nonuniformity can alter device performance and reliability. In order to improve interfacial quality, such processing procedures as two-step oxidation process (12-13) and post-oxidation annealing (14-15) have been proposed. Both methods include annealing of the grown oxides in a nonoxidizing atmosphere such as argon or nitrogen. High-resolution TEM was used to investigate the influence of the annealing on interface smoothness (12-13, 16), but the results are ambiguous and on some points contradictory. Yet there seems to be general agreement that annealing improves both electronic properties and interface flatness.

Spectroscopic ellipsometry has been applied to study interfaces under transparent films(17), and recently we reported an interface enhanced immersion spectroscopic technique(18), which is sensitive to such interface characteristics as microroughness, thickness and phase composition. In the present study we apply this new method

to determine the properties and reactions at the Si/SiO₂ interface during the post-oxidation annealing.

Experimental Procedures and Data Analysis

Single-crystal (100) oriented 2 Ω cm p-type silicon wafers were cleaned using a slightly modified RCA procedure (19) and thermally oxidized in a fused silica tube furnace in clean dry oxygen to about 24-27 nm SiO₂ at 800°C. Upon completion of a particular oxidation one sample was removed without annealing as a control and the others were annealed in a clean nitrogen atmosphere. We used annealing temperatures and times in the range 750-1100°C and 1-120 min, respectively.

In order to investigate the Si/SiO₂ interface we have applied a novel enhanced sensitivity spectral and variable angle of incidence immersion ellipsometry technique (18). The key feature of this technique is that spectroscopic and variable angle of incidence ellipsometry measurements are performed in a transparent liquid ambient that has optical properties very close to the those of the SiO₂ overlayer. Therefore, the overlayer film is "optically" (not physically) eliminated and the probing light beam becomes highly sensitive to the interface properties.

Generally it is difficult to achieve a perfect refractive index match for the liquid ambient, n_o , and the SiO₂ overlayer, n_{ov} , over a broad spectral range. Therefore deviations are accounted for in the analysis(18).

Carbon tetrachloride (CCl₄) is a suitable immersion liquid for

matching index to SiO₂ films. The refractive index of the liquid ambient, n_o , was calculated from a Cauchy dispersion formula, taking into account temperature:

$$n_o = n_\infty + \frac{a}{\lambda^2} + \frac{\partial n}{\partial T} \Delta T \quad (1)$$

where λ in Å is the wavelength of probing beam, parameters $n_\infty = 1.4427$, $a = 5.15 \times 10^5 \text{Å}^2$ at $T=24.8^\circ\text{C}$ (20) and $\partial n/\partial T=0.00055$ at $T=20^\circ\text{C}$ for pure CCl₄ (21).

It is known that the refractive index of thin-film SiO₂ overlayers, n_{ov} , depends on thickness, L_{ov} , oxidation temperature, T_{ox} , annealing temperature, T_m , and time, t_m , index of the substrate orientation, N , and preparation conditions such as preoxidation cleaning and oxidation ambient. The spectral dependence of the non-annealed thin-film SiO₂ refractive index, $n_{ov}^o(L_{ov}, T_{ox}, \lambda)$, for a substrate with particular orientation, e.g (100), was calculated from a single term Sellmeier approximation:

$$n_{ov}^o(L_{ov}, T_{ox}, N, \lambda) = 1 + \frac{A(L_{ov}, T_{ox}, N) \lambda^2}{\lambda^2 - \lambda_o^2(L_{ov}, T_{ox}, N)} \quad (2)$$

where $A(L_{ov}, T_{ox}, N)$ and $\lambda_o(L_{ov}, T_{ox}, N)$ are dispersion parameters that are also dependant on the overlayer thickness and preparation conditions and with values $A=1.15$ and $\lambda_o=92.3$ nm for 25-35 nm thick thermally grown at 800°C on Si(100) SiO₂ films (10).

It has been observed that the refractive index of the SiO₂ overlayer undergoes a relaxation during annealing (22-25). Ellipsometric measurements of the thermal relaxation of the SiO₂

single film effective refractive index, i.e. without taking the interface into consideration, shows (23) that two relaxation processes are involved: rapid (~10-20 min.) initial relaxation and slow exponential decay to the refractive index of fully relaxed oxide. The slow exponential decay is because of the elastic strain relaxation and well described as:

$$n_{ov}(L_{ov}, T_{ox}, T_{an}, t_{an}, N, \lambda) = n_f(\lambda) + [n_{ov}^o(\lambda) - n_f(\lambda)] \exp\left(-\frac{t_{an}}{\tau}\right)^\eta \quad (3)$$

where n_f is the refractive index for fully relaxed oxide, and the empirical parameter $\eta=0.17$ (22), which is a measure of the strength of the coupling between the index and relaxation. The relaxation time for the oxide density is expressed as:

$$\tau(T_{an}) = \tau_o \exp\left(\frac{E_o}{kT_{an}}\right) \quad (4)$$

where $\tau_o \sim 2 \times 10^{-23}$ min and $E_o \sim 6$ eV (22). We have assumed that the refractive index of the fully relaxed oxide film is equal to that for the bulk oxide, and thus the spectral dependence $n_f(\lambda)$ was calculated with eqn.(2) using $A=1.099$ and $\lambda_o=92.27$ (10) which corresponds to bulk SiO_2 . The observed initial rapid relaxation of the effective refractive index (23) can be attributed to the evolution of the interface, and a detailed model for this will be discussed below.

In order to obtain unknown interface parameters, we used a Marquardt non-linear best fit algorithm which minimizes the value of the error function:

$$Q = \sum_{i,j} [(\Delta_{i,j}^{cal}(\phi_i, E_j, P) - \Delta_{i,j}^{exp})^2 + (\Psi_{i,j}^{cal}(\phi_i, E_j, P) - \Psi_{i,j}^{exp})^2] \quad (5)$$

where P is a vector of unknown interface parameters, E_j is the photon energy, ϕ_i is the angle of incidence, and the subscripts cal and exp refer to calculated and experimentally derived values. Δ^{cal} and Ψ^{cal} are the values obtained using the vector P from expanded Fresnel formulas (26) and a matrix algorithm for the multilayer system with optical parameters for the CCl_4 ambient and SiO_2 overlayer calculated from the eqns.(1-4) and the previously determined thickness of the SiO_2 overlayer. The Bruggeman effective medium approximation (27), BEMA, was used to calculate the effective dielectric function of the interface, which was modeled as a mixture of constituents (discussed later) with known optical properties. Volume fractions of the constituents were calculated from assumptions about the geometry of the interface that are discussed below, and the geometrical parameters have been included as unknown parameters.

A commercially available vertical ellipsometer bench was modified to become a rotating analyzer spectroscopic ellipsometer (the essential features were previously described (28)) and calibrated according to a published procedure (29). A specially designed variable angle of incidence immersion cell that fits on the ellipsometer stage was used (18). For each sample spectroscopic ellipsometry was performed both in air and CCl_4 in the 2.4-4.0 eV range of photon energies, E , and at two angles of incidence, ϕ , of 72° and 75° . The measurements yield the

ellipsometric angles $\Delta^{exp}(E, \phi, T_m, t_m)$ (Fig.1) and $\Psi^{exp}(E, \phi, T_m, t_m)$ as a function of annealing conditions (T_m, t_m) . As was previously discussed (18) the sensitivity of Ψ to interface changes is considerably less than for Δ , hence only Δ is used to correlate with process changes. From the measurements done in air, the thickness of the SiO_2 overlayer was obtained without significant error, because there is very low interface sensitivity for the measurements in air (18).

In order to obtain interface dependencies, which characterize the evolution of the interface via annealing, we have calculated an effective relative interface parameter:

$$\delta\Delta_{int}(T_{an}, t_{an}) = \Delta^{exp}(T_{an}, t_{an}) - \Delta_o^{exp} - \delta\Delta_{ov}^{cal}(T_{an}, t_{an}) \quad (6)$$

where $\Delta^{exp}(T_m, t_m)$ is the experimental ellipsometric angle Δ at an annealing temperature and time, Δ_o is the ellipsometric angle for a non-annealed sample and the term $\delta\Delta_{ov}^{cal}(T_m, t_m)$ is the overlayer relaxation correction. This correction term represents the difference in Δ for the single-film (without interface) system of a non-annealed and annealed overlayer with the refractive index calculated from eqns.(2-4). The chosen photon energy $E=3.18$ eV is in the range of the maximum interface and the minimum overlayer sensitivity (18).

Results and Discussion

I. Model Independent Results

Firstly, Fig. 1 shows that $\Delta^{cp}(E, \phi, T_m, t_m)$ is measured with enhanced sensitivity at different annealing conditions in the spectral energy range 2.8-3.4 eV. Figures 2 and 3 display experimental results in terms of the interface parameter $\delta\Delta_{int}(T_m, t_m)$ defined by eqn.(6) above. Thus Figs. 2 and 3 show the values for $\delta\Delta_{int}$ measured at 3.18 eV versus anneal time at a number of temperatures in Fig. 2, and versus anneal temperature at two times in Fig. 3. Other information relating to modelling is also included in Fig. 3, but discussion of these items will be deferred to later sections. It is seen in Fig. 2 that at all annealing temperatures two temporal regions of behavior are present. Initially, the anneals yield a fast increase in $\delta\Delta_{int}$ that slows quickly after 5 min and then nearly saturates. Taking the data from Fig. 2 at two anneal times, one before and one near saturation, and plotting versus anneal temperature reveals a distinct break in the 900°-970°C range, which corresponds to the viscous flow range, i.e. a temperature above which viscous flow of the oxide is fast (30). Thus we consider that the viscous relaxation dominates at the higher anneal temperatures, but at lower temperatures we need to consider other possible mechanisms. It is clear that the low temperature mechanism accounts for a large part of the change in $\delta\Delta_{int}$.

If the interface region is treated as a single homogenous film, then the extent of the interface is observed to decrease with both annealing time and temperature as evidenced by the increasing Δ_{int} . With both a decrease in the interface region for short and

long times and low and high temperatures the models that are chosen for the different modes of behavior must show the same characteristics.

II. A Working Model for the Si-SiO₂ Interface.

The transition from crystalline Si, c-Si, to bulk amorphous SiO₂ includes at least two physically distinct regions. First there is a short range decay region from the c-Si in which the long-range crystalline order of c-Si disappears, i.e. the memory of the Si order is lost. The characteristic range for this zone is 0.1-2 nm. Second, there is a longer range decay region possibly extending to tens of nm into the amorphous SiO₂ where mechanical stress, density and refractive index relax to the bulk SiO₂ values. Annealing decreases the extent of both regions. One way to think about the interface between film and substrate is as a transition region that has a structure with two major components each with a substructure: the "physical" interface and the "chemical" interface. The "physical" interface consists of a mixture of substrate and overlayer constituents, which can represent microroughness or protrusions of Si into the oxide and even inclusions of SiO₂ microcrystallites, such as cristobalite or tridymite (10). This layer represents an order transition. The "chemical" interface consists of a new chemical compound with a wide homogeneity range, a suboxide, SiO_x, with $0 < x < 2$. In the chemical interface we permit other properties such as stress, density and refractive index

(which are likely related (24) to relax to bulk values.

For the purpose of analyzing the experimental data in terms of physical parameters, we propose a model for the interface consisting of these two distinct entities: the physical and chemical interfaces. The physical interface is modeled as Si protrusions whose distribution and size are important parameters. The chemical interface is modeled as a suboxide that coats the physical interface. Fig. 4 shows a sketch of our model. Below we provide the parameters that quantify this working model, and then the experimental data $\Delta^{exp}(E, \phi, T_m, t_m)$ and $\psi^{exp}(E, \phi, T_m, t_m)$ from Figs. 2 and 3 are reduced to yield values for the model parameters which are compared with other studies about the interface region. Finally, we discuss the mechanisms that could diminish both interfaces with annealing, since that is what we observe. It should be understood that our model is a "working" model based on many presently available research results. While we show good agreement between the parameters obtained in this model and independent measurements on the interface region, we do not prove our model but only further demonstrate its reasonableness, and more importantly provide physically relevant parameter changes related to the condition of the interface such as surface roughness and stoichiometry.

We describe the crystalline silicon protrusions as hemispheres with an average radius R , which form a hexagonal network with an average distance D between centers of the protrusions. Thus the

protrusions define the "physical" interface with a thickness R . The protrusions and the region between them are covered by a layer of suboxide SiO_x , $0 < x < 2$, with an average thickness L_{so} . This layer forms a chemical transition zone from Si to SiO_2 , or the "chemical" interface. It is possible to model both the "physical" and the "chemical" interfaces as one transition layer with an effective thickness:

$$L_{int} = R + L_{so} \quad (7)$$

and an effective dielectric function ϵ_{int} , which represents a mixture of crystalline silicon c-Si, silicon suboxide SiO_x and the SiO_2 overlayer and written as:

$$\epsilon_{int} = \epsilon_{int}(\epsilon_{c-Si}, f_{c-Si}, \epsilon_{\text{SiO}_x}, f_{\text{SiO}_x}, \epsilon_{\text{SiO}_2}, f_{\text{SiO}_2}) \quad (8)$$

ϵ_{int} was calculated using the BEMA, where the dielectric properties, ϵ , and relative volume fractions, f , of all of the interfacial layer constituents are known a priori. The dielectric function of SiO_x was calculated using the BEMA, and by considering that SiO_x is a mixture of amorphous silicon, a-Si, and SiO_2 (38). The relative volume fractions of Si-Si and Si-O bonds, $f_{\text{Si-Si}}$ and $f_{\text{Si-O}}$, respectively, are:

$$f_{\text{Si-Si}} = \frac{2-x}{2+x}, \quad f_{\text{Si-O}} = \frac{2x}{2+x} \quad (9)$$

The refractive index of the SiO_2 overlayer was calculated from eqns.(2-4). The relative volume fractions of the interfacial layer constituents f_{c-Si} , f_{SiO_x} and f_{SiO_2} were calculated from the assumed geometry of the interface and given as:

$$f_{c-si} = \frac{4\pi R \rho^2}{3\sqrt{3}(R+L_{so})}, \quad \rho = \frac{R}{D}$$

and

(10)

$$f_{sio_x} = \frac{L_{so}}{R+L_{so}} \left(1 + \frac{2\pi \rho^2}{\sqrt{3}} \right), \quad f_{sio_2} = 1 - f_{c-si} - f_{sio_x}$$

In order to model the evolution of the interface during annealing, we use a power law to describe the reduction of both the protrusions (physical interface) and the chemical transition layer (chemical interface):

$$R = R^o - \alpha(T_{an}) t_{an}^p$$

and

(11)

$$L_{so} = L_{so}^o - \beta(T_{an}) t_{an}^g$$

where R^o and L_{so}^o are, respectively, initial values for the average radius of the protrusions and for the thickness of the chemical transition layer. The kinetic coefficients $\alpha(T_m)$ and $\beta(T_m)$ are annealing temperature dependent factors related to the rate limiting processes discussed below. The powers p and g are taken to be $p=g=0.5$ which is model dependent and justified below based on diffusion.

The minimization of the error function (eqn.(5)) for the sets of experimental data for the non-annealed wafer at $\phi=72^\circ$ and 75° with fitting parameters D , R^o and L_{so}^o (at $x=1$) gives the average distance between the centers of protrusions $D = 44 \pm 4 \text{ \AA}$, initial

radius of the protrusions $R^0 = 9.8 \pm 0.3 \text{ \AA}$ and initial thickness of suboxide SiO $L_{\text{so}} = 3.4 \pm 0.2 \text{ \AA}$. These results are in agreement with the interface geometry sensitive TEM study of the $\text{SiO}_2\text{-Si}$, which shows that distances between protrusions at non-annealed interface are distributed in the range 40-50 \AA and heights are 9-15 \AA (1,2). Also, photoelectron spectroscopy revealed a chemical transition layer with a thickness of 2.4-4 \AA (11, 44).

A simulation of the kinetic dependencies, $\delta\Delta_{\text{int}}(T_{\text{an}}, t_{\text{an}})$, using eqns. (7,9-11) with $p=g=0.5$ yields the coefficients $\alpha(T_{\text{an}})$ and $\beta(T_{\text{an}})$ as functions of t_{an} or T_{an} as is shown in Fig. 5. At annealing temperatures less than 900°C the kinetic coefficient $\beta(T_{\text{an}})$, which characterizes the "chemical" interface evolution, is negligibly small and, therefore, the "chemical" interface is stable. The kinetic coefficient $\alpha(T_{\text{an}})$ describing the "physical" interface evolution or the silicon protrusions diminution, is saturated and becomes temperature independent at T_{an} in the range of 850-950°C. The comparison of the experimental plots of $\delta\Delta_{\text{int}}(t_{\text{an}})$ with simulations (dashed lines in Fig. 2) shows good agreement. Note, that the asymptotic form assumed for the interface reduction laws given as eqn. (11), at $t_{\text{an}} \gg 1$ is incorrect, since it leads to a disappearance of the interface region after sufficient time of annealing. Nevertheless, the phenomenological model satisfactorily describes the experimental curves of Figs. 2 and 3 for tens of minutes and reflects the main features of the process.

Figure 6 displays the decrease of the extent of the interface, i.e. effective thickness from eqn. (7) with a minimum thickness of

about 3 Å realized at the highest anneal temperatures. The interface effective refractive index vs t_m at several T_m is shown in Fig.7. Initially both the index and thickness of the interface layer decrease due to the shrinking of the silicon protrusions. This is followed by the slower decrease of the SiO_2 transition layer which becomes dominant after considerable reduction of the height of the protrusions. The sharp increase in the index seen in Fig. 7 for the 1100°C annealed sample is indicative of the index returning quickly to the SiO value as the fraction of the Si as protrusions in the interface layer rapidly goes to zero. The same effect would occur for the other anneal temperatures but more slowly. A slower rise in index is seen for the 1050°C annealed sample after 10 min and the time is too short to see the rise for the lower temperature anneals. The overall shape of the results in Fig. 7 is typical of and dictated by the BEMA model used to interpret the data.

Discussion of the Interface Model

We have considered two interface regimes that decrease with annealing. The physical interface is typified by the Si protrusions that decrease in size and number during annealing. The driving force for this is the minimization of the interfacial free energy that requires an increase in the radius of curvature for interface protrusions or a reduction of the interface area covered by the protrusions with decreasing radius, thereby reducing the interface width. The chemical interface is typified by the

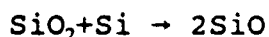
suboxide and is reduced by the conversion of suboxide due to the presence of oxygen which produces SiO_2 or the evaporation of suboxide or to both, and by the relaxation of interfacial stress. The interfacial stress can also couple into the reduction of the physical interface by providing an additional driving force for the migration of atoms to reduce the protrusions. We discuss the viscous flow and interface reaction components of the interface annealing mechanism separately.

Viscous Flow Mechanism. In the Si-SiO₂ system there is considerable evidence that stress relaxation occurs at high temperature by viscous flow (22, 24-25, 31) with a viscous flow point for bulk SiO₂ near 950°C (23-24, 30). Stress relaxation by viscous flow decreases the oxide density with a relaxation time τ expressed by eqn.(4). The characteristic relaxation time, τ , is of the order of a few minutes at 1000°C and a few hours at 900°C (22-24, 30). This strongly suggests that the viscous flow mechanism may be dominant at temperatures higher than ~950°C, but becomes negligible at lower temperatures and for annealing times less than ~1 hour, i.e. the short annealing times of the present study. Furthermore, the temperature activated exponential nature of a viscous flow mechanism is not evident in Figs 3 and 5 for temperatures below 950°C, but is in evidence in this data at the higher anneal temperatures. From Fig. 3, we observe that at $T_m < 900^\circ\text{C}$, $\delta\Delta_m(T_m)$ (at constant time of annealing) tends to saturation, and the kinetic coefficients $\alpha(T_m)$ and $\beta(T_m)$ are saturated at $T_m = 900-950^\circ\text{C}$ (Fig.5).

Yet, at these lower temperatures significant change also occurs in the interface as evidenced in Figs 2 and 3. At high temperatures the migration of Si from the protrusions occurs via two driving forces: free energy and stress. Another low temperature mechanism dictates the interface changes at low temperatures and we consider that the chemical reactions at the interface are likely important.

Interfacial Chemical Reaction Mechanism. The reduction of both the physical and chemical interface can occur by the reduction in available Si at the interface. Above, the diffusion of Si atoms from the protrusions in response to the thermodynamic and mechanical forces was considered. However, it is difficult to understand how the chemical interface can be reduced by this mechanism, since Si from SiO_2 or SiO is not readily available to migrate.

Thermal dissociation of SiO_2 has received recent attention (32-34). It was shown that at elevated temperatures and with an oxygen deficiency (vacuum or an inert gas ambient) the SiO_2 decomposition takes place via an interface reaction (32):



At temperatures $T_m > \sim 900^\circ\text{C}$ voids are formed at the interface after long-term vacuum annealing. The kinetics of the void growth (32) demonstrates that the oxide decomposition reaction is initiated at active defect sites already present at the Si/SiO_2 interface.

Annealing at $\sim 750-900^{\circ}\text{C}$ which is insufficient for void growth, transforms these defects into an electrically active state which seem to cause low-field dielectric breakdown (33,37). The Si protrusions cannot be excluded from consideration as defects that could cause the above SiO_2 disproportionation, since these sites are thermodynamically active owing to the smaller radius of curvature. It is noteworthy that Walkup and Raider (43) did not observe the escape of SiO during defect formation and indeed the diffusion of SiO in SiO_2 would likely not be a favored process. However, if dissolved traces of oxygen or water are present, in the overlying SiO_2 and/or in the anneal ambient, this available oxidant might remove SiO through formation of SiO_2 . In our experiments we have used pure anneal gases and careful procedures. However, our anneal systems are open flowing systems and our gases are from tanks. Thus trace amounts of oxidants are present and can be dissolved and accumulated in the SiO_2 . It was shown (33) that with sufficient O_2 (ppm level) present during inert gas annealing, O_2 reoxidizes SiO at the defects and prevents the low-field breakdown. This chemistry may lead to a gradual reduction of the active defect sites and causes the saturation of $\delta\Delta_m(T_m, t_m)$ at $T_m < 900^{\circ}\text{C}$ seen in Fig.3. From this data in the low temperature region it can be argued that a reduction both of O_2 concentration in the interface layer and the active sites due to oxidation could be a rate-limiting factor.

In the anneal temperature region $900^{\circ} < T_m < 970^{\circ}\text{C}$ both mechanisms, viz. relaxation and chemical reaction are in evidence. We have assumed that the interfacial diffusion of atoms is a limiting

process for the evolution of both the "physical" and the "chemical" interface. At high temperatures ($T_m > 950^\circ\text{C}$) the "physical" interface changes by the diffusion of Si atoms away from protrusions and viscous flow of SiO_x (or SiO_2) in the opposite direction. At 1000°C the viscous flow relaxation time is a few minutes, but as seen in Fig.2 the interface continues to change for longer times with a slower rate. After the fast and ample reduction of the extent of the physical interface for $t_m \sim 10$ min, the interface evolves slowly (with $\beta \ll \alpha$) by the reduction of the chemical interface via the interfacial diffusion-limited reactions of decomposition and oxidation of suboxide. At moderate temperatures ($T_m < 900^\circ\text{C}$) the decrease of SiO_x ($x \leq 2$) is diffusion limited (36) likely by the diffusion of oxidant through the silica network to the interface. Thus, it was reasonable to use a diffusional square-root time law for the "physical" and "chemical" interface evolution, i.e. $p=q=0.5$, and a good fit was found. According to the model developed here, annealing in an oxidant free atmosphere at low temperatures, where the reoxidation reaction $2\text{SiO} + \text{O}_2 \rightarrow 2\text{SiO}_2$ cannot take place will result in no annihilation of the electrically active sites.

Conclusions

A novel enhanced interface sensitivity immersion spectroscopic ellipsometry technique was applied to study the Si/ SiO_2 interface annealing. Two distinct stages of interface evolution were found: a fast initial stage with interface microroughness reduction

followed by a slow decay of the interfacial suboxide. The interfacial suboxide reoxidation reaction dominates the interface evolution in the moderate temperatures region ($T_m < 900^\circ\text{C}$) and viscous flow becomes dominant at elevated temperatures ($T_m > 950^\circ\text{C}$).

Acknowledgments

This research was supported in part by the Office of Naval Research, ONR.

REFERENCES

1. A.H.Carim and R.Sicclair, Mater. Lett, 5, 94 (1987).
2. N.M. Ravindra, D.Fathy, J.Narayan, J.K.Srivastava, and E.A.Irene, J. Mater. Res., 2, 216 (1987).
3. I.W.Boyd and J.I.B.Wilson, J. Appl. Phys., 62, 3195 (1987).
4. P.O.Hahn and M.Henzler, J. Appl. Phys., 52, 4122 (1981).
5. A.H.Carim, M.M.Dovec, C.F.Quate, R.Sinclair, and C.Vorst, Science, 237, 630 (1987).
6. E.A.Taft and L.Cordes, J. Electrochem. Soc., 126, 131 (1979).
7. D.E.Aspnes and J.B.Theeten, J. Electrochem. Soc., 127, 1359 (1980).
8. A.Kalnitsky, S.P.Tay, J.P.Ellul, S.Chongsawangvirod, J.A.Andrews, and E.A.Irene, J.Electrochem. Soc., 137, 234 (1990).
9. V.Nayar, C.Pickering, and A.M.Hodge, Thin Solid Films, 195, 185 (1991).
10. G.E.Jellison, Jr., J. Appl. Phys., 69, 7627 (1991).

11. F.J.Grunthaner and P.J.Grunthaner, Chemical and Electrical Structure of the SiO_2/Si Interface, Elsevier/North Holland, Amsterdam, 1987.
12. A.Bhattacharyaa, C.Vorst, and A.H.Carim. J. Electrochem. Soc., 132, 1990 (1985).
13. N.M.Ravindra, D.Fathy, J.Narayan, J.K.Srivastava, and E.A.Irene. Mater. Lett., 4, 337 (1986).
14. A.H.Carim and A.Bhattacharyaa, Appl. Phys. Lett., 46,872 (1985).
15. M.H.Hecht, L.D.Bell, F.J.Grunthaner, and W.J.Kaiser, Mat. Res. Soc. Symp. Proc., 105, 307 (1988).
16. A.Ogura, J. Electrochem. Soc., 138, 807 (1991).
17. D.E.Aspnes, J. Vac. Sci. Technol., 18, 289 (1981).
18. V.A.Yakovlev and E.A.Irene. Submitted in J. Electrochem. Soc.
19. W.Kern and D.A.Puotinen, RCA Rev., 31, 187 (1970).
20. P.Perez, T.E.Block, and C.M.Knobler, J. Chem. and Engineering Data, 16, 333 (1971).

21. "Techniques of Chemistry", Ed. A. Weissberger, Vol.II Organic Solvents, Ed. J.A. Riddick and W.B. Bunger, Wiley Interscience, NY,1970.
22. K.Taniguchi, M.Tanaka, C. Hamaguchi, and K.Imai, J. Appl. Phys., 67, 2195 (1990).
23. L.M.Landsberger and W.A.Tiller, Appl. Phys. Lett., 51, 1416 (1987).
24. E.A.Irene, E.Tierney, and J.Angillelo, J. Electrochem. Soc., 129, 2594 (1982).
25. E.Kobeda and E.A.Irene, J. Vac. Sci. Technol. B, 5, 15 (1987).
26. R.M.A.Azzam and N.M.Bashara, Ellipsometry and Polarized Light, North-Holland, Amsterdam, 1977.
27. D.E.Aspnes, Thin Solid Films, 89, 249 (1982).
28. X.Liu, J.W.Andrews, and E.A.Irene, J. Electrochem. Soc., 138, 1106 (1991).
29. J.M.M. de Nijs, A.H.M.Holstlag, A.Hoeksta, and A. van Silfhout, J. Opt. Soc. Am., A,5, 1466 (1988).

30. E.P.EerNisse, Appl. Phys. Lett, 35, 8 (1979)
31. A.H.Carim and R.Sinclair. J. Electrochem. Soc., 134, 741 (1987)
32. R.Tromp, G.W.Rubloff, P.Balk, F.K.LeGoues, and E.J.van Loenen. Phys. Rev. Lett., 55, 2322 (1985).
33. G.W.Rubloff, K.Hoffmann, M.Liehr, and D.R.Young. Phys. Rev. Lett., 58, 2379 (1987).
34. R.E.Walkup and S.I.Raider. Appl. Phys. Lett., 53, 889 (1988).
35. G.K.Celler and L.E.Trimble. Appl. Phys. Lett., 53, 2493 (1988).
36. G.K.Celler and L.E.Trimble. Appl. Phys. Lett., 54, 1427 (1989).
37. M.Arienzo, L.Dori, and T.M.Szabo, Appl. Phys. Lett., 49, 1040 (1986).
38. G.Zuther, Phys. St. Sol.(a), 59, K109 (1980).
39. L.Dori, J.H.Stathis, and J.A.Tornello, J. Appl. Phys., 70, 1510 (1991).
40. E.A.Irene and R.Ghez, Appl. Surf. Sci., 30, 1 (1987).

41. M.Niwano, H.Katakura, Y.Takeda, Y.Takakuwa, N.Miyamoto, A.Hiraiwa, and K.Yagi, J. Vac. Sci. Technol. A 9, 195 (1991).
42. I.Ohdomari, H.Akatsu, Y.Yamakoshi, and K.Kishimoto, J. Appl. Phys., 62, 3751 (1987).
43. R.E.Walkup and S.I.Raider, Appl. Phys. Lett., 53, 888 (1988).
44. T.Hattori and T.Suzuki, Appl. Phys. Lett., 43, 470 (1983)

FIGURE CAPTIONS

Figure 1. The experimental dependence of the ellipsometric angle, Δ , on photon energy, E , at different annealing times.

Figure 2. The experimental dependence of the effective interface parameter, Δ_{int} , on annealing time at a number of annealing temperatures. A simulated dependency is shown with the dashed curve.

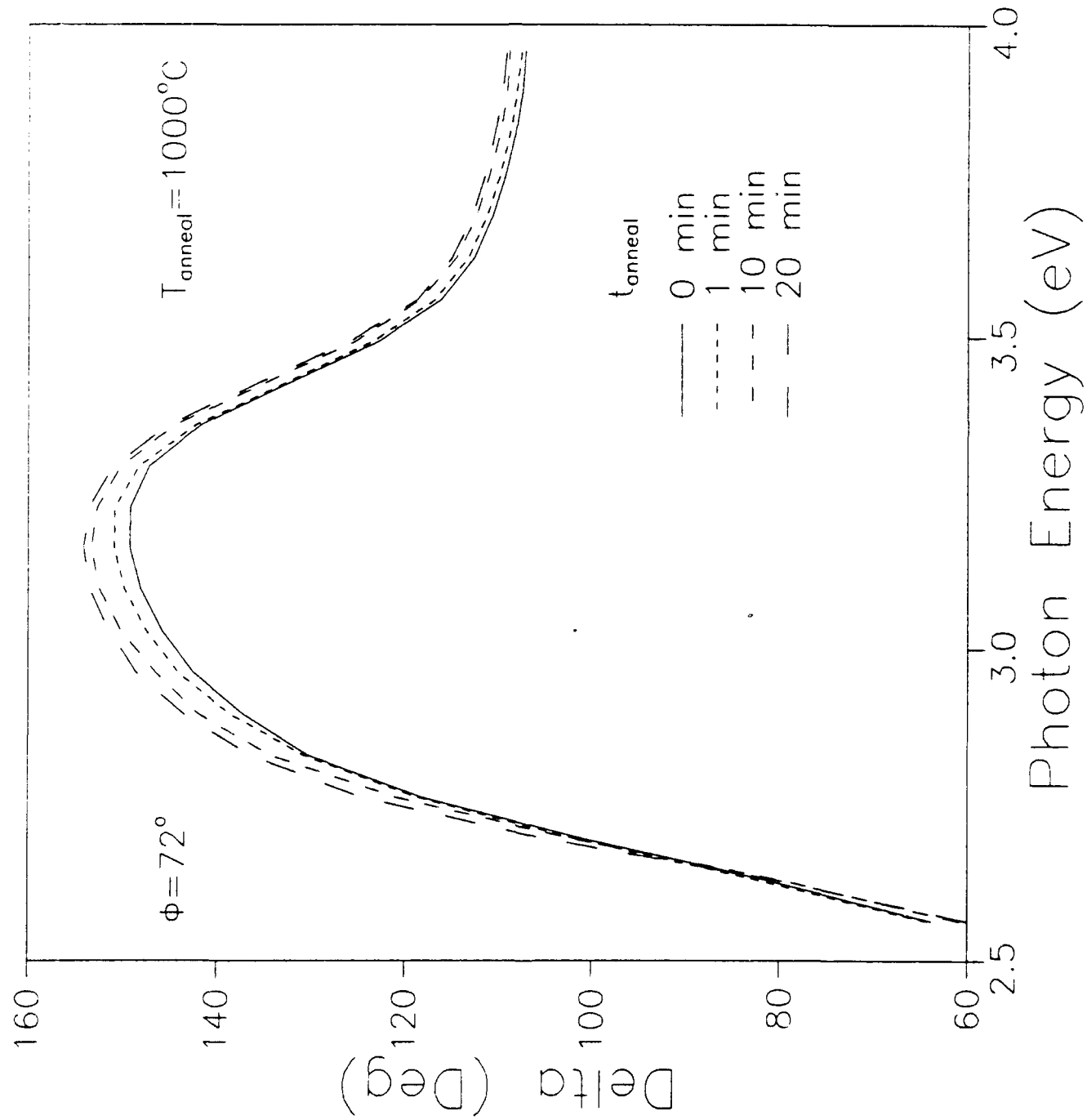
Figure 3. The experimental dependence of the effective interface parameter, Δ_{int} , on annealing temperature for two annealing times.

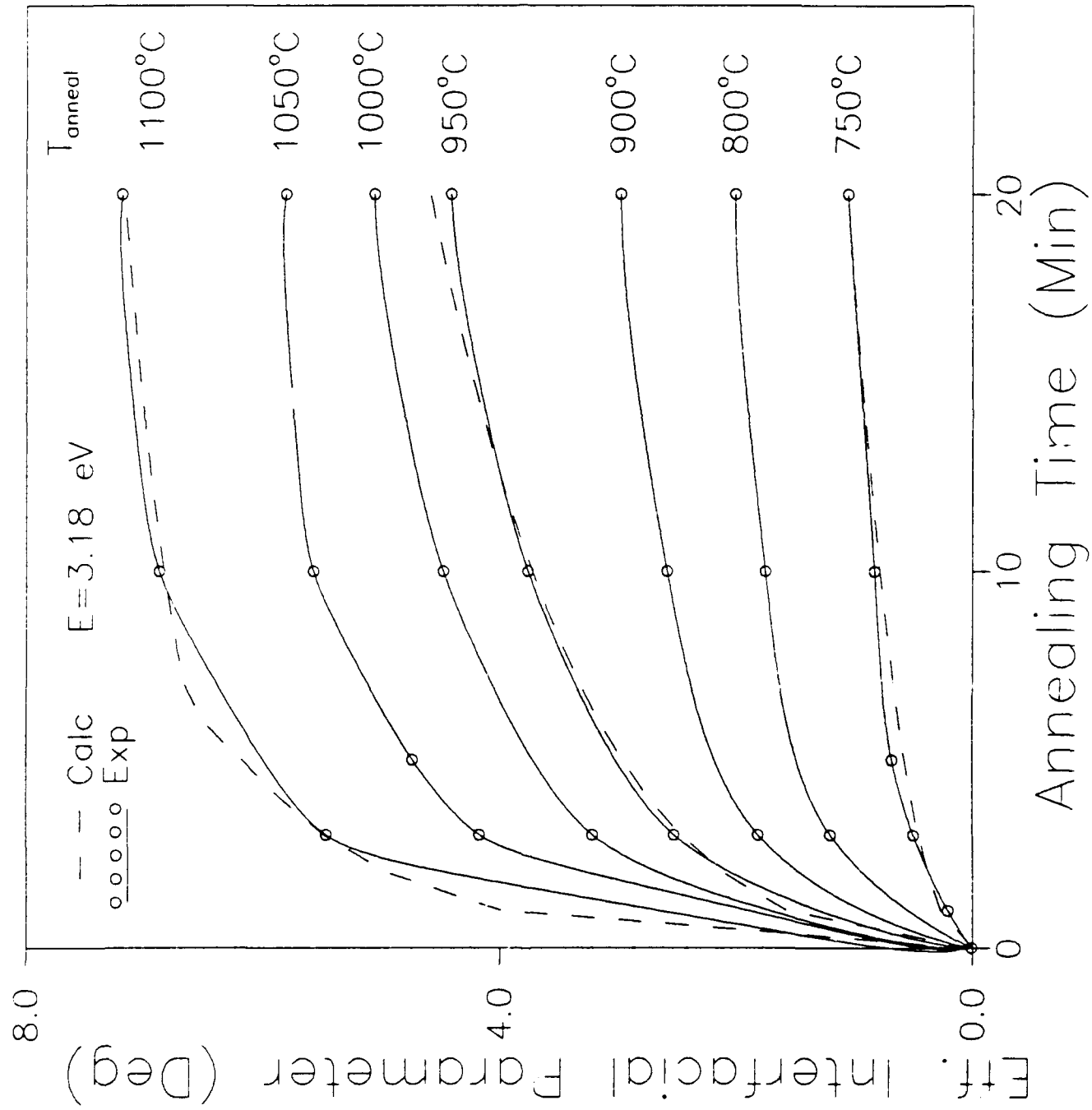
Figure 4. Schematic representation of our interface model.

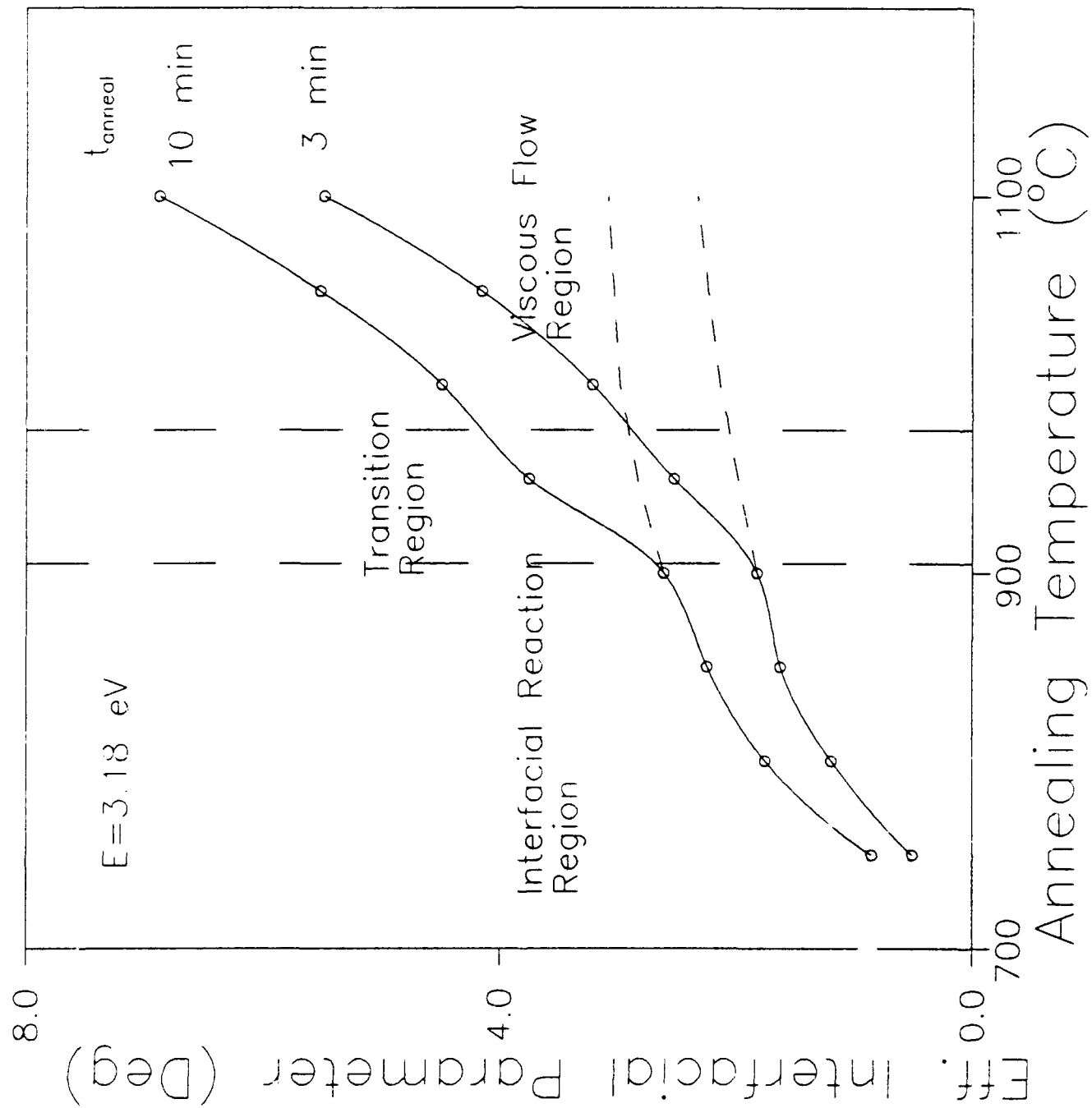
Figure 5. The dependence of the kinetic coefficients α and β on annealing temperature.

Figure 6. The dependence of the effective interface thickness on annealing time at a number of annealing temperatures.

Figure 7. The dependency of the effective interface refractive index on annealing time at a number of annealing temperatures.







Interface Model

